

FABRICATION AND TESTING OF A PROTOTYPE RF-DIPOLE CRABBING CAVITY*

S. U. De Silva[†], J. R. Delayen, Old Dominion University, Norfolk VA, USA
 H. Park¹, Thomas Jefferson National Accelerator Facility, Newport News VA, USA
¹currently at Fermi National Accelerator Laboratory, Batavia IL, USA

Abstract

Crabbing cavities are essential in particle colliders to compensate the luminosity degradation due to beam collision at a crossing angle. The 952.6 MHz 2-cell rf-dipole crabbing cavity system was proposed for the Jefferson Lab Electron-Ion Collider to restore the head-on collisions of electron and proton bunches at the interaction point. A prototype cavity was designed and developed to demonstrate the performance of multi-cell rf-dipole structures. This paper presents the fabrication process and cold test results of the first 2-cell rf-dipole prototype cavity.

INTRODUCTION

Advanced high energy particle colliders are currently being developed with high peak luminosities to study properties of particles in the Standard Model. These powerful colliders require higher rate of particle interactions between bunches to achieve the desired integrated luminosities over the duration of machine operation. The higher beam energies also require large crossing angles to minimize the beam interactions where the two beams share the same vacuum space. The reduction of luminosities due to large crossing angles are compensated by the implementation of crabbing systems at the interaction region [1]. The crabbing cavities provide a transverse kick to the head and tail of each bunch that will oscillate the bunches such that they overlap at the interaction point in maximizing the number of interactions between them.

Jefferson Lab Electron-Ion Collider

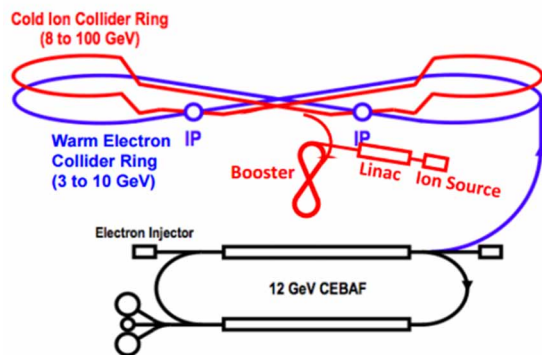


Figure 1: Schematic of Jefferson Lab Electron-Ion Collider.

* This material is based upon work supported by a grant from the Southeastern Universities Research Association (SURA). This research also used resources of the National Energy Research Scientific Computing Center (NERSC); a U.S. Department of Energy Office of Science User Facility operated under Contract No. DE-AC02-05CH11231.

[†] sdesilva@jlab.org

Jefferson Lab Electron-Ion Collider (JLEIC) was a next generation particle collider designed to be built at Jefferson Lab [2]. In parallel, another Electron-Ion Collider (EIC) was proposed by BNL [3]. JLEIC was designed to accelerate electrons in the existing CEBAF accelerator with a newly constructed figure-8 ring to accelerate protons and ions as shown in Fig. 1. The collider will consist of two interaction points with a luminosity goal in the range of low-to-mid 10^{33} cm⁻²sec⁻¹ per interaction point. The crab cavities are required to achieve the luminosity goal and are designed to operate at 952.6 MHz [4].

Following the site selection process in early 2020, BNL was selected as the site for the next EIC and JLEIC project was discontinued. This paper presents the details of the rf design, fabrication and rf testing of a prototype crabbing cavity that was designed and developed for the JLEIC.

RF DESIGN

The rf-dipole design is a compact crabbing cavity design that operates in a TE₁₁-like mode where the primary contribution to the transverse kick is provided by the transverse electric field across the pole gap [5,6]. Single cell rf-dipole cavities have been designed and developed for several deflecting and crabbing applications at 400 MHz, 499 MHz, 750 MHz [7]. Higher operating frequencies allow compact geometries as the cavity diameter is inversely proportional to the frequency. Multiple cavity geometries of squashed elliptical, 1-cell, 2-cell and 3-cell rf-dipole design options were evaluated at 952.6 MHz frequency and the 2-cell rf-dipole design was finalized as the crab cavity design for JLEIC [8,9].

Figure 2 shows the 2-cell rf-dipole cavity and cross section with the cavity dimensions. The cavity was designed with the beam aperture of 70 mm and center to center pole separation of 170 mm $> \lambda/2 = 157.4$ mm. The pole height and angle are optimized to reduce peak surface fields and to achieve a balance B_p/E_p ratio. Figure 3 shows the surface field profiles, and Table 1 lists the rf properties.

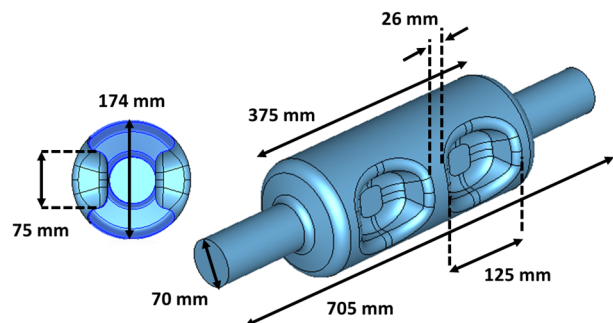


Figure 2: 952.6 MHz 2-cell rf-dipole cavity.

Content from this work may be used under the terms of the CC BY 4.0 licence (© 2023). Any distribution of this work must maintain attribution to the author(s), title of the work, publisher, and DOI

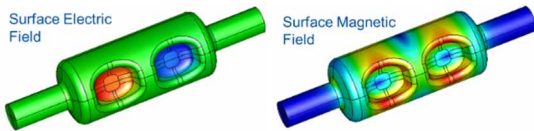


Figure 3: Surface electric (left) and magnetic (right) of the 2-cell rf-dipole cavity.

Table 1: RF Properties of the 2-Cell RF-Dipole Cavity

| Property | Value | Units |
|---------------------------------|-------------------|------------|
| f_0 | 952.6 | MHz |
| Similar Order Mode (SOM) | 849.7 | MHz |
| Nearest HOM | 1395.4 | MHz |
| Peak electric field (E_p^*) | 5.74 | MV/m |
| Peak magnetic field (B_p^*) | 11.72 | mT |
| B_p^* / E_p^* | 2.04 | mT/(MV/m) |
| Geometrical factor (G) | 171.3 | Ω |
| $[R/Q]_r$ | 149.3 | Ω |
| $R_t R_s$ | 2.6×10^4 | Ω^2 |

* At $E_t = 1$ MV/m

PROTOTYPE CAVITY FABRICATION

The 2-cell rf-dipole cavity is fabricated with RRR Nb as shown in Fig. 4. The cavity is fabricated with 3 sub-assemblies consisting of the center body and 2 end caps welded together with beam tube assemblies. The center body consists of two 2-pole sections and 2 strips welded together.

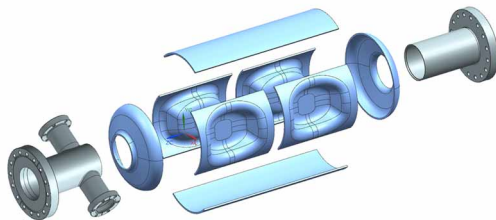


Figure 4: Exploded view of the 2-cell rf-dipole cavity.

The detailed fabrication process is listed below:

- Stamping dies shown in Fig. 5 are used to form the individual poles and the end caps.



Figure 5: Forming dies for end caps (top) and pole (bottom).

- End caps and all the poles are formed first using Al 6061 sheet cut outs. After finalizing the blank shapes, the Nb parts are formed with 1/8" thick Nb sheets as shown in Fig. 6. Beam tubes are rolled using forming dies and welded at the Electron Beam Welding (EBW) machine at JLab.



Figure 6: Formed poles, end caps and beam tubes.

- After forming the end caps are trimmed at the iris to the desired length to be welded to the beam tube assemblies.
- Beam pipe assemblies are completed by brazing the Nb beam tube with SS CF flanges. The side ports are welded on one of beam pipe assemblies (Figure 7).



Figure 7: Beam pipes assemblies.

- Individual poles are trimmed on one side and welded together as shown in Fig. 8.



Figure 8: Welded poles.

- The strips for the center body were rolled and trimmed to be welded with the poles. The 4 parts in the center body were aligned to maintain the symmetry and correct pole separation. A disk type fixture was used to clamp the parts together and tack welded first before completing the full welds (Figure 9).
- After the welding, the center body was trimmed to clean the edges while maintaining the symmetry along

the axis. The center body length was limited due to slightly shorter strip parts.



Figure 9: Center body welding in the EBW machine.

- The welding edges of the final 3 subassemblies were machined to a uniform thickness of 2.5 mm for a depth of 4 mm. The parts were aligned before machining to achieve matched weld profiles between the parts.
- A detailed surface inspection was carried out and several locations were polished using a grinding tool to remove dents on the surface.
- The final welding of the end cap to the center body was completed in two passes and repeated for the second end cap as shown in Fig. 10. Figure 11 shows the final welded cavity.



Figure 10: Final welding of the 2-cell rf-dipole cavity.



Figure 11: Final welded 2-cell rf-dipole cavity.

CAVITY PROCESSING AND ASSEMBLY

The 2-cell rf-dipole cavity was processed, assembled and rf tested at Jefferson Lab. The cavity processing steps are listed below:

- Ultrasonic degreasing
- Thickness measurements before bulk BCP
- Bulk BCP of 120 μm
- Thickness measurement after bulk BCP
- Heat treatment at 600 $^{\circ}\text{C}$ for 10 hours
- Light BCP of 30 μm . Actual removal – 25 μm

- Thickness measurements after light BCP
- High pressure rinsing (HPR) of 2 passes with cavity flipped after the 1st pass
- Cavity assembly, evacuation, and leak test in the clean room
- Low temperature bake (LTB) at 120 $^{\circ}\text{C}$ for 48 hours

The 2-cell cavity bulk BCP is carried out at Jefferson Lab BCP cabinet as shown in Fig. 12. The two 2 $\frac{3}{4}$ " CF side ports were blanked, and acid was circulated through the two beam ports. The target removal was 120 μm and actual removal is 108 μm . Similarly, the target removal for light BCP was 30 μm and actual removal is 25 μm . The cavity was degreased prior to HPR and was rinsed in 2 passes. Post rinsing cavity was dried in clean room for ~24 hours prior to assembly. The cavity was assembled in the clean room at Jefferson Lab with rf test probes, then evacuated to be tested in a Vertical Test Assembly (VTA).



Figure 12: 2-cell cavity in BCP cabinet (top), HPR cabinet (middle), and bake box for LTB (bottom).

RF TESTING

The 2-cell rf-dipole cavity assembly include input test probe inserted at one of the side ports and field probe inserted at the opposite beam pipe. Both input and field probes are coaxial antennas, and the field probe was off-centered to be coupled to the electric field. The cavity was assembled with 8 thermal sensors near high magnetic field regions and on the poles where electric field is maximum.

The cavity was tested at both 4 K and 2 K. The frequency at 2 K is 960.0 MHz, which is off by 7 MHz. The contribution to frequency shift is possibly due to shorter length in the center body and wider pole gap. A detailed metrology measurement of the cavity center body is planned to be completed.

Multipacting Analysis

The multipacting resonances for the 2-cell rf-dipole cavity were analysed using Track3P code in the SLAC ACE3P suite [10]. The primary particles are generated on 1/8th of the cavity volume and then traced for 50 rf cycles. The impact energies of the resonant particles are shown in Fig. 13. The location of the resonant particles on the cavity surface and the corresponding impact energies and transverse voltages are shown in Fig. 14. Similar to single cell rf-dipole cavity geometries the resonant particles are seen on the end plates of the cavity and on the top and bottom of the cavity.

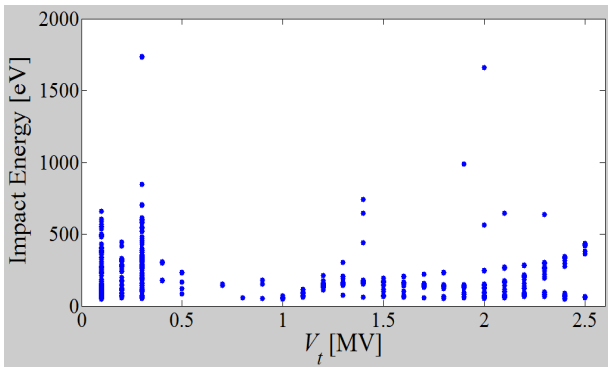


Figure 13: Impact energy vs V_t of the 2-cell rf-dipole cavity.

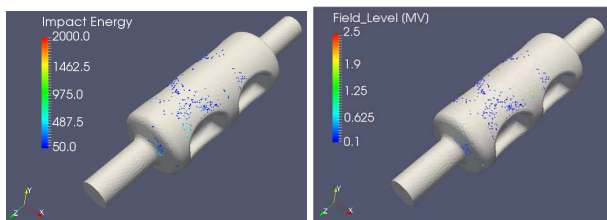


Figure 14: Location of the resonant particles for different impact energies (left) and transverse voltage (right) for the 2-cell rf-dipole cavity.

Initially multipacting resonances at very low transverse voltages were processed at 4 K. Data were taken around 0.35 MV during cavity cool down up to 2 K to determine the residual surface resistance of the cavity. Figure 15 shows the fitted surface resistance as a function of $1/T$. The estimated residual surface resistance is 28.5 n Ω . The BCS

resistance at 960 MHz is ~ 9.4 n Ω . The surface resistance corresponds to a low field Q_0 of $\sim 5 \times 10^9$ as seen in the 2 K test.

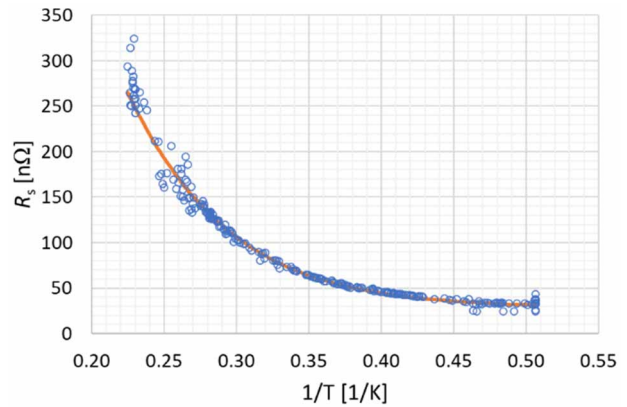


Figure 15: Surface resistance of the 2-cell cavity.

RF Test at 2.0 K

The cavity showed multipacting resonances at a barrier around 0.5 MV, which matches with the simulation data shown in Fig. 13. Therefore, the cavity was cooled down to 2.0 K to further process multipacting resonances. Figure 16 (blue curve) shows the multipacting resonances on the cavity. The multipacting resonances were not fully processed in the cavity after several hours of processing.

At higher voltages (orange curve) no multipacting was observed and the cavity achieved a Q_0 of $\sim 10^{10}$ with a maximum transverse voltage of 3.35 MV. The cavity didn't quench and was limited by the allowable power rating on the input power cable. No significant radiation was observed at higher transverse voltages. Multipacting resonances was seen again as the transverse voltage was reduced. The cavity showed a lower Q_0 (grey curve). This is possibly due to field emitter burn out and was not able to recover the Q_0 , which limited the maximum transverse voltage to 2.25 MV.

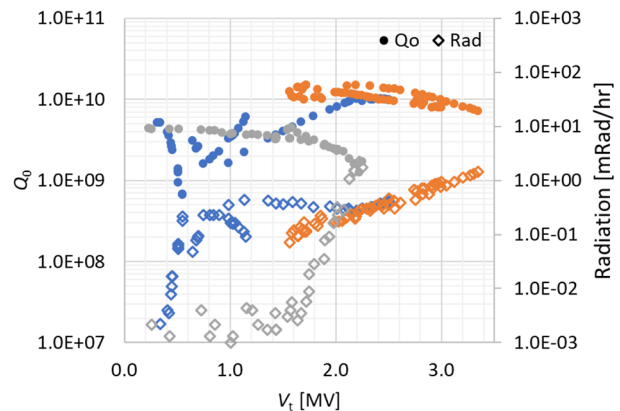


Figure 16: Q_0 vs V_t of the 2-cell prototype cavity.

The cavity was thermal cycled by increasing the temperature to 30 K and cooling down to 2 K. The Q_0 did not improve as shown in Fig. 17. Multipacting was observed around 0.5 MV. The final peak fields achieved by the cavity are $E_p = 54.3$ MV/m and $B_p = 96.5$ mT.

Content from this work may be used under the terms of the CC BY 4.0 licence (© 2023). Any distribution of this work must maintain attribution to the author(s), title of the work, publisher, and DOI

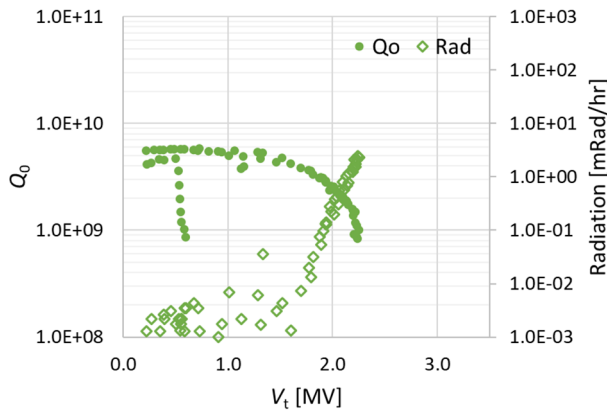


Figure 17: Q0 vs Vt after thermal cycling.

A preliminary surface inspection was carried out after the rf tests and residue on one of the end caps were noticed. A thorough surface inspection will be carried out followed by a full cycle of BCP etching and processing.

CONCLUSION

A 2-cell rf-dipole cavity has been designed, fabricated and rf tested, in demonstrating the performance of multi-cell high frequency rf-dipole deflecting/crabbing cavities. The cavity fabrication followed the standard fabrication techniques of superconducting Nb cavities. The cavity fabrication was carried out to achieve the frequency as is built, therefore, additional fixturing was not used in maintaining desired pole gap. The target frequency at 2 K was 952.6 MHz and the measured cavity frequency at 2 K was 960.0 MHz. The ~7 MHz frequency is caused possibly due to the shorter center body length and wider pole gap. A detailed metrology scan will be carried out to determine the dimensions of the fabricated cavity along with bead pull measurements. The cavity was tested at 2 K and was required to process multipacting barriers at a transverse voltage range of 0.5–1.5 MV for several hours. The cavity achieved a maximum transverse voltage of 2.25 MV corresponding to peak fields of 54.3 MV/m and 96.5 mT.

REFERENCES

- [1] R. B. Palmer, “Energy Scaling, Crab Crossing, and the Pair Problem”, SLAC, CA, USA, Rep. SLAC-PUB-4707, Jun. 1988.
- [2] S. Abeyratne *et al.*, “MEIC Design Summary”, January 2015. doi:10.48550/arXiv.1504.07961
- [3] S. U. De Silva, J. R. Delayen, J. Guo, Z. Li, R. A. Rimmer, and B. P. Xiao, “197 MHz Waveguide Loaded Crabbing Cavity Design for the Electron-Ion Collider”, in *Proc. NAPAC’22*, Albuquerque, NM, USA, Aug. 2022, pp. 679-682. doi:10.18429/JACoW-NAPAC2022-WEPA26
- [4] S. U. De Silva, J. R. Delayen, and H. Park, “Multi-Cell RF-Dipole Deflecting and Crabbing Cavity”, in *Proc. IPAC’16*, Busan, Korea, May 2016, pp. 2469-2471. doi:10.18429/JACoW-IPAC2016-WEPMW022
- [5] S. U. De Silva and J. R. Delayen, “Design evolution and properties of superconducting parallel-bar rf-dipole deflecting and crabbing cavities”, *Phys. Rev. Accel. Beams*, vol. 16, p. 012004, 2013. doi:10.1103/PhysRevSTAB.16.012004
- [6] S. U. De Silva and J. R. Delayen, *Phys. Rev. Accel. Beams*, “Cryogenic test of a proof-of-principle superconducting rf-dipole deflecting and crabbing cavity”, vol. 16, p. 082001, 2013. doi:10.1103/PhysRevSTAB.16.082001
- [7] S. U. De Silva, A. Castilla, and J. R. Delayen, “Compact Superconducting RF-dipole Cavity Designs for Deflecting and Crabbing Applications”, in *Proc. IPAC’13*, Shanghai, China, May 2013, paper WEPWO080, pp. 2483-2485. <https://jacow.org/IPAC2013/papers/WEPWO080.pdf>
- [8] H. Park, A. Castilla, S. U. De Silva, J. R. Delayen, and V. S. Morozov, “Analyses of 476 MHz and 952 MHz Crab Cavities for JLAB Electron Ion Collider”, in *Proc. IPAC’16*, Busan, Korea, May 2016, pp. 2348-2350. doi:10.18429/JACoW-IPAC2016-WEPMR034
- [9] S. U. De Silva, J. R. Delayen, and H. Park, “Higher Order Multipole Analysis for 952.6 Mhz Superconducting Crabbing Cavities for Jefferson Lab Electron-Ion Collider”, in *Proc. IPAC’17*, Copenhagen, Denmark, May 2017, pp. 1177-1179. doi:10.18429/JACoW-IPAC2017-MOPVA136
- [10] Z. Li, L. Ge, C.-K. Ng, and L. Xiao, “Recent Developments and Applications of Parallel Multi-Physics Accelerator Modeling Suite ACE3P”, in *Proc. NAPAC’19*, Lansing, MI, USA, Sep. 2019, pp. 888-891. doi:10.18429/JACoW-NAPAC2019-WEPL04

Content from this work may be used under the terms of the CC BY 4.0 licence (© 2023). Any distribution of this work must maintain attribution to the author(s), title of the work, publisher, and DOI